

A general formulation of eutectic silicon morphology and processing history

J. E. Spinelli ^{a,b(1)}, W. Hearn ^b, A-A. Bogno ^b, and H. Henein ^b

^a Department of Materials Engineering, Federal University of São Carlos, São Carlos, SP 13565-905 Brazil.

^b Department of Chemical and Materials Engineering, University of Alberta, Edmonton, AB T6G 2G6 Canada.

Keywords: Coupled-zone, Undercooling, Al-Si, Microstructure, Cooling Rate, Thermal History.

Abstract

Understanding the influence of rapid solidification conditions on the formed microstructure is important to determine how process conditions affect the final mechanical properties. In this work the rapid solidification of hypoeutectic and hypereutectic Al-xSi (x=10wt. %, 18wt %) alloys was achieved using Impulse Atomization (IA). The resultant microstructures were examined and from this analysis a wide range of eutectic Si morphologies and length scales were observed. These results were further analyzed using 2 mathematical approaches to help quantify the experienced eutectic growth kinetics (i.e. growth rate and cooling rate) and thermal history of the powders. In the case of the hypereutectic Al-Si alloy distinct microstructure zones were observed. These distinct zones were used to determine the nucleation undercooling using combined concepts of the coupled zone in Al-Si alloys and the hypercooling limit of a melt. Here, a region of fine eutectic, α -Al+Si, is observed and is believed to be the first solids that precipitated directly from the undercooled melt and grew during recalescence. Following recalescence, a coarser structure of Si particles and eutectic developed. The solidification paths of both hypo and hypereutectic Al-Si alloys will be outlined and a generalized approach to relate the shape of the eutectic Si to processing conditions will be presented.

1. Introduction

Al-Si alloys are of great interest in industry [1-3] due to their favorable castability, wear resistance, corrosion resistance, strength and weldability [4-6]. A good portion of these properties are directly related to the solidification microstructures of Al-Si, specifically the eutectic structure, as it accounts for 50-90% of the total volume formed in these alloys.

The equilibrium microstructures of hypereutectic Al-Si alloys consist of primary Si crystals enveloped in a (α -Al+Si) eutectic mixture [3,7]. While for hypoeutectic Al-Si alloys the equilibrium microstructures consist of primary α -Al crystals enveloped in the (α -Al+Si) eutectic mixture [8]. The proportion of eutectic depends on the nominal composition of the alloy as well as the thermal history during solidification. If the system is far from the thermodynamic equilibrium conditions (i.e. fast cooling conditions), kinetically modified eutectic structures can be expected. For example, in the analysis of Al-18wt.%Si powders generated by gas atomization, Kalay and collaborators [9] observed microstructural transitions from dendrites to cells and from cells to microcells as the experienced cooling rate increased.

The Al-Si system exhibits a skewed coupled zone [10], and has a wide variety of microstructures that can form which depend on the composition, solidification velocity and thermal history. Trivedi and co-authors [10] have described the influence of these conditions on the formed microstructure of rapidly solidified Al-Si alloys by developing a growth rate-composition map. In this map the coupled zone was shown to shift from a symmetrical position to one that is skewed towards the facet-forming Si side of the phase diagram (i.e., towards the hypereutectic side) [11, 12]. This means that for eutectic and hypereutectic alloys, critical growth rates seem to exist beyond which eutectic solidification is not possible for eutectic composition and eutectic structure prevails for hypereutectic chemistries.

A continuing challenge involving solidification studies is predicting the formed microstructure that stems from specific processing conditions. This is even more challenging when examining rapid solidification processes.

¹ Corresponding author: E-mail address: spinelli@ufscar.br (J.E.Spinelli)

Formulations taking into account features of Al-Si, such as the morphology of the eutectic Si related to local solidification conditions (i.e., solidification velocity, V and thermal gradient, G), could be of interest for those involved in rapid solidification techniques such as fusion casting, powder metallurgy and spray deposition [13,14].

In the case of Al-Si alloys, several models and approaches have been developed over the last six decades [15-18]. These models determine the interfacial undercoolings and solidification velocities using the eutectic Si spacing (λ). Eutectic modeling of Al-Si has seen a lot of changes over the years, from the classical description by Jackson and Hunt [18] given as early as 1966, to the modified eutectic theory for irregular growth as more recently covered by Gunduz *et al.* [19]. The formation of irregular eutectic structure, initially described by Toloui and Hellawell [20], is characterized by the tendency of Si flakes to grow in a specific direction only, so that the neighbouring plates will either diverge or converge. If there is convergence, growth stops when the λ becomes smaller than a critical spacing (extremum spacing). In the case where a diverging flake prevails, another critical spacing (maximum spacing) governs the growth process. When this spacing is achieved, the growth becomes unstable and one of the flakes branches out into two diverging flakes, thereby reducing the spacing. Although the referred models and theories have proven to be useful for a number of applications, expansion of their predictive capabilities are still needed to encompass a broader range of processing parameters, sizes and morphologies in Al-Si alloys.

Few studies have focused on correlating the microstructure and morphologies of Al-Si alloys, with the growth kinetics defined by solidification parameters such as cooling rate, undercooling or growth rate. Therefore, a systematic study of microstructure evolution of controlled rapid solidified Al-Si powders would provide a reliable quantitative knowledge of the relationship between solidification parameters and microstructural scale.

This paper investigates microstructural evolutions in both hypoeutectic Al-10Si and hypereutectic Al-18Si powders generated by Impulse Atomization (IA). Particularly, the evolution of the eutectic structure within these rapidly solidified powders is examined. The thermal history is inferred based on a combination of experimental findings along with various analytical approaches. Broad processing diagrams, showing maps in G_E - V_E space with the eutectic Si morphology, are proposed.

2. Materials and methods

2.1. Powder production

Al-10wt.%Si and Al-18wt.%Si alloys were produced by induction melting in a graphite crucible, using a mixture of commercial purity Al (99.9%) and high purity Si (99.99%) for the Al-10wt.%Si and a mixture of high purity Al (99.99%) & Si (99.99%) for the Al-18wt.%Si. Powders of size ranging from $<75 \mu\text{m}$ to $1000 \mu\text{m}$ were then generated by IA in both argon and helium atmospheres. Detail description of the process is given elsewhere [21]. In the present work powders of size ranges (in μm) <75 , 90-106, 106-125, 212-250, 300-355 and 425-500 will be investigated.

2.2. Analytical tools

X-ray diffraction (XRD) analysis was carried out to identify the precipitated phases, using a Rigaku Geigerflex Powder Diffractometer, within an angular range varying from 10° to 120° (2θ) with a step-size of 0.02° and a dwell time of 0.6 s per step. The current and the voltage of the X-ray tube were 38 mA and 38 kV, respectively. The radiation was $\text{Co } K\alpha$ with a wavelength of 1.78899 \AA .

Metallographic analysis was performed to reveal the microstructural and morphological details of the eutectic Si, using grinding and polishing steps in combination Keller's reagent. Micrographs were obtained using a motorized BX61 Olympus optical microscope and a Zeiss Sigma Field Emission SEM equipped with a Bruker energy dispersive X-ray spectroscopy (EDS) system with dual silicon drift detectors each with an area of 60 mm^2 and a resolution of 123 eV. The SEM analysis was carried out in both Secondary Electrons (SE) and In-Lens detector modes.

The measurement of eutectic Si spacing (λ), for both the hypo and hypereutectic compositions, was obtained using the line intercept method [22]. The λ for the Al-18wt.%Si was determined as a function of position moving from the nucleation point towards the particle's surface. Here, a total of 6 values of λ were measured at 6 different positions for each investigated powder cross section.

3. Results and discussions

3.1. Microstructures formation and processing history

Fig.1 shows the XRD patterns of the samples from both hypo and hypereutectic compositions and from different size ranges. The diffraction patterns, as expected, were indexed to the solid solution phase (α -Al – major phase) plus Si for both compositions.

As expected, the hypoeutectic alloy microstructures consist of primary α -Al surrounded by the (α -Al+Si) eutectic structure (Fig.2a). It can be seen that a bit farther away from the nucleation region (Fig. 2a₂) the eutectic Si is a bit coarser than that in the area associated with the proposed nucleation (see Fig. 2a₁).

And, the hypereutectic alloy overall microstructures in Fig. 2b consist of two distinct zones, A and B (details in Fig.2b₁ and Fig. 2b₂, respectively). Zone A, consisting of a eutectic structure (α -Al+Si), appears to be the primary solidification microstructure and is characterized by a finer scale, while Zone B is coarser and consists of elongated primary Si particles surrounded by the eutectic structure. The relative fraction of each microstructural zone was determined by image analysis of the micrographs. Zone A is found to increase with decreasing powder size. It worth noting that, the primary solidification of the undercooled hypereutectic Al-18wt% Si is expected to be an eutectic structure as the primary nucleation temperature falls within the coupled zone of the Al-Si system as described by Trivedi *et al.* [10]. Zone A is assumed to have formed adiabatically during recalescence so that the primary nucleation undercooling, ΔT_N , can be estimated as a function of the volume fraction of zone A, F_R , the melt heat capacity, C_p^l , and the latent heat of fusion, ΔH_f (Equation (1)) [23]. $C_p^l = 920.0 \text{ J/(kg.K)}$ and $\Delta H_f = 397,300 \text{ J/kg}$ for Al-Si [24,25].

$$\Delta T_N = F_R \times \frac{\Delta H_f}{C_p^l} \quad (1)$$

The estimated average values of ΔT_N for all the investigated Al-18Si powders increases as the powder size decreases (increasing cooling rate). These values are found to be lying within the coupled zone region of the Al-Si system as shown in Fig. 3.

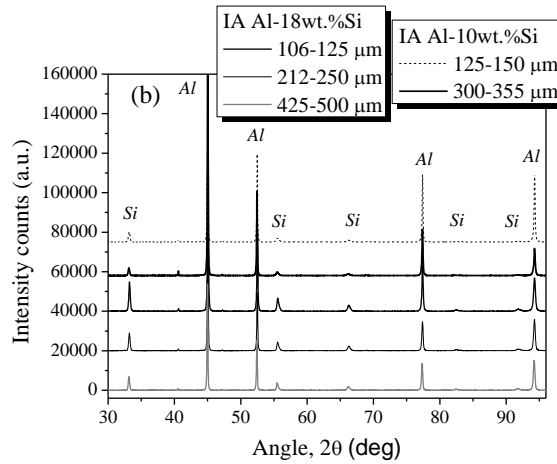


Fig. 1: XRD patterns of hypo and hypereutectic Al-Si powders generated by impulse atomization (IA): Al-10wt.%Si powders atomized in argon and helium respectively and Al-18wt.%Si alloys atomized in helium.

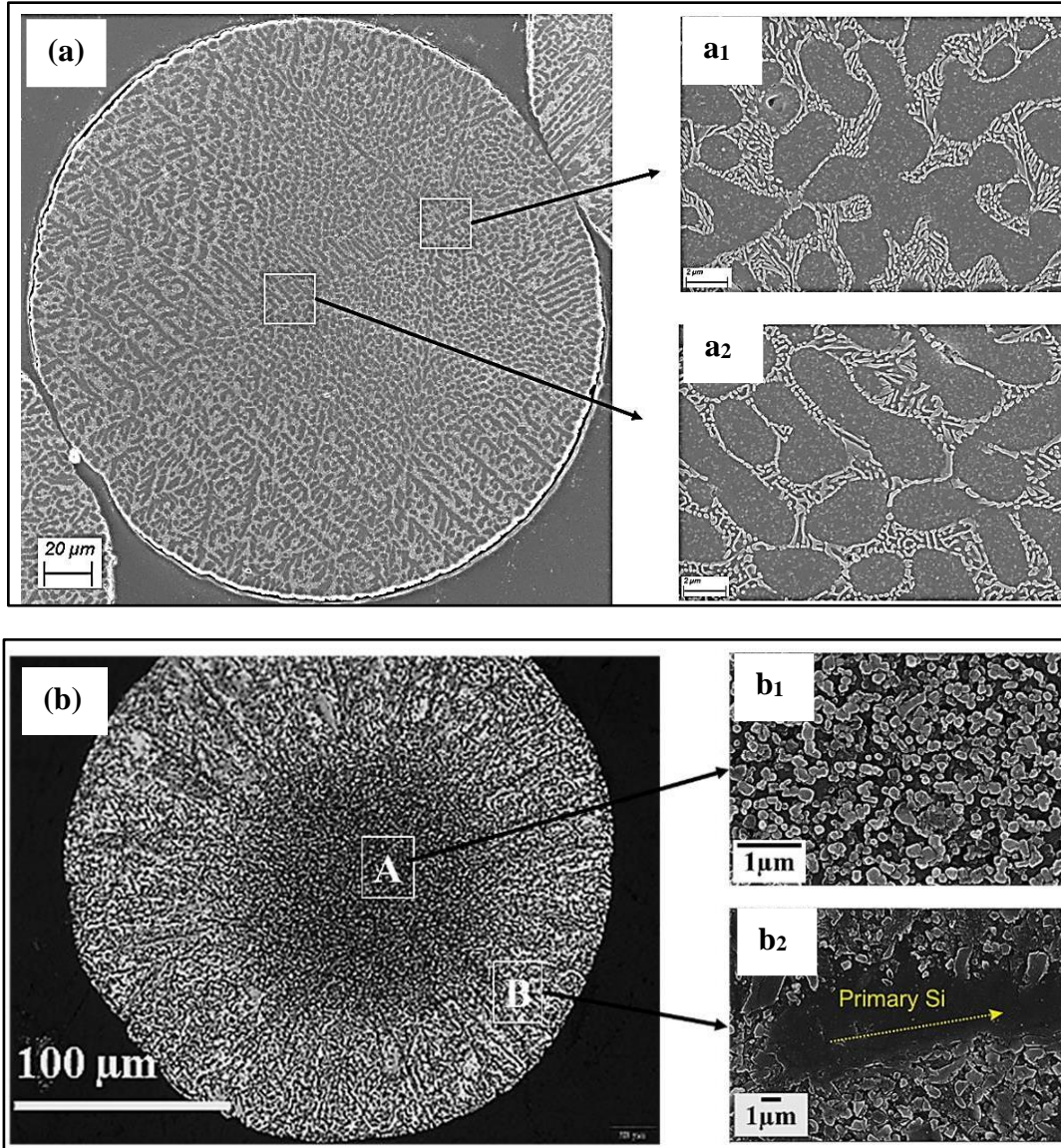


Fig. 2: (a) Optical micrograph of a typical Al-10wt.%Si alloy powder microstructure of the size range 212-250 μm , produced by IA in helium. (a₁, a₂) SEM images detailing different portions of this particle. (b) Optical micrograph of a typical Al-18wt.%Si alloy powder microstructure produced by IA in helium, within the size range 212-250 μm . (b₁,b₂) High magnification SEM images of a portion of the zone A (eutectic $\alpha\text{-Al}+\text{Si}$) and the zone B (elongated Si + coarse eutectic), respectively. The arrow in (b₂) indicates the growth direction of the primary Si.

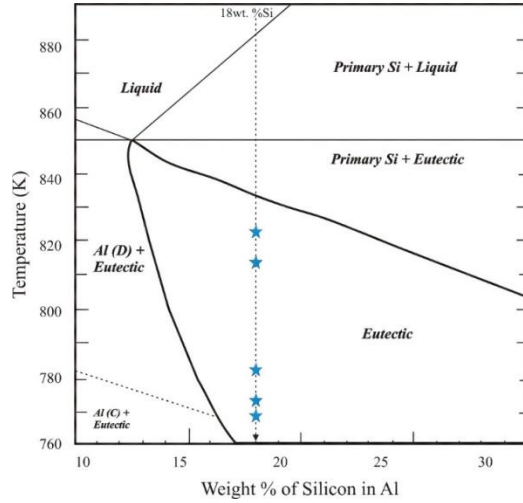


Fig. 3: Al-Si phase diagram showing the primary nucleation undercooling, ΔT_N (stars symbols) of IA Al-18wt% Si powders generated in helium. The values are found to be lying within the predicted coupled zone of the system [diagram adapted from 10].

In order to investigate the eutectic growth mechanism in both hypo and hypereutectic powders, the growth rate, V , which depends on the interface undercooling, ΔT , was determined as a function of the average Si interparticle spacing λ using a modification of the Jackson and Hunt eutectic growth model for irregular growth (Equations (2) [18]. The used ϕ coefficient is a dimensionless operating parameter that helps describe irregular eutectic growth and is equal to 2.3 for the Al-Si eutectic [17].

$$\lambda^2 V = \frac{\phi K_2}{K_1} \quad (2)$$

K_1 and K_2 are described by Gunduz in [26] and the defining physical properties for the Al-Si eutectic can be found in [9, 24, 25, 27, 28].

Fig.4 shows the typical variation of V_{JH} (J-H Velocity) with the relative positions across the microstructures for Al-18wt%Si alloy powders. As can be seen, the interface velocity decreases along the growth direction from the nucleation to the surface.

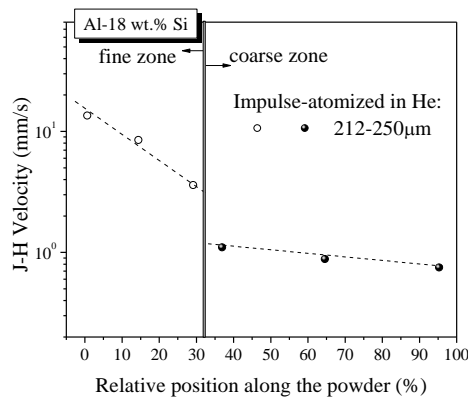


Fig. 4: Typical interface velocity evolution (Jackson-Hunt velocity), V , as a function of the relative position along the Al-18wt.%Si alloy powder for the the size range 212-250 μm .

Fig.5 shows the variation of λ with V_{JH} . As expected, λ decreases with increasing V_{JH} . These results are in good agreement with the results obtained by other researchers for hypo and hypereutectic Al-Si solidified under different conditions, including stationary regime and gas-atomization [9, 17, 26]. The agreement with the literature results shows that the application of the modified Jackson-Hunt approach for Al-Si is justified.

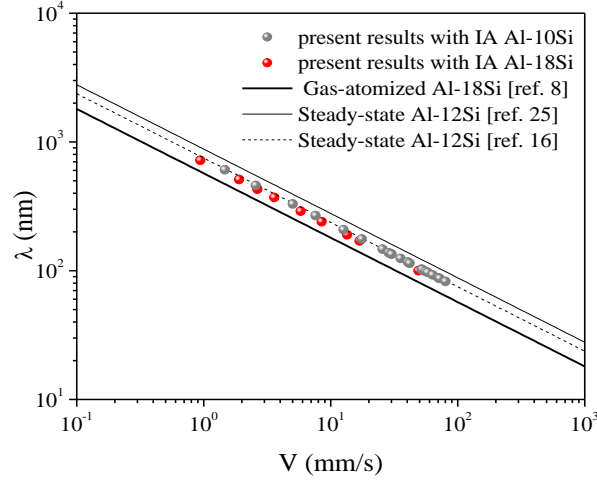


Fig. 5: Variation of the Si interparticle spacing λ with the interface velocity V during rapid solidification of the Al-10 (gray) and 18 wt.%Si (red) powders generated by IA (round symbols). These experimental results are compared with three literature results (line plots) [9, 17, 26].

The interface cooling rate, CR , is estimated using Equation (3), which is the result of an analytical thermal analysis for the unidirectional solidification of metals in a casting, developed by Garcia et al [29] and adapted to a spherical particle.

$$k \left(\frac{dT}{dr} \right)_{r=r_f} = \Delta H_f d \left(\frac{d_{r_f}}{dt} \right) \quad (3)$$

Where k and d are respectively the thermal conductivity and the density of the liquid, dr is an incremental solid layer as solidification advances; and r_f is the radius of the freezing eutectic front. The thermal energy per time in the right side of the Equation (3) must be equal to the energy transported by conduction (left side). Based on Equation (3) a relationship between the eutectic cooling rate, CR (also defined as $G_E \times V_E$) and growth rate V_E can be expressed as in Equation (4).

$$CR = C_1 V_E^2 \text{ or } CR = C_1 V_{JH}^2 \quad (4)$$

Where C_1 defined by $(\Delta H_f \times d)/k$ is an alloy composition dependent term. The value of C_1 is experimentally found (as the slope of the linear fitting of CR Vs V_E^2) to be $1.6 \times 10^7 \text{ K.s.m}^{-2}$ by Reyes et al [3] which is in agreement with the theoretical value of $1.5 \times 10^7 \text{ K.s.m}^{-2}$.

Thus, CR could be obtained at different positions x_i along the growth direction, from the nucleation point towards the surface of a powder.

3.2 Si morphologies variation of the eutectic Si

Fig. 6a and Fig. 6b show the typical variation in Si morphology, due to growth kinetics (expressed in terms of powder size, atomization gas and λ), for Al-10wt% Si and for Al-18wt% Si. As can be seen in the inserted SEM

microstructures, the Si morphology varies from elongated/fibrous to round/globular as the cooling rate increases for both compositions. This variation is characterized by a decrease in powder size, along with using helium instead of argon, for the Al-10wt% Si alloy powder. And is characterized by using a point close to the nucleation zone along with a point close to the surface for the Al-18wt% Si alloy powder. These observations suggest that the solidification kinetic parameters, CR , V_E and G_E affect the morphology of Si.

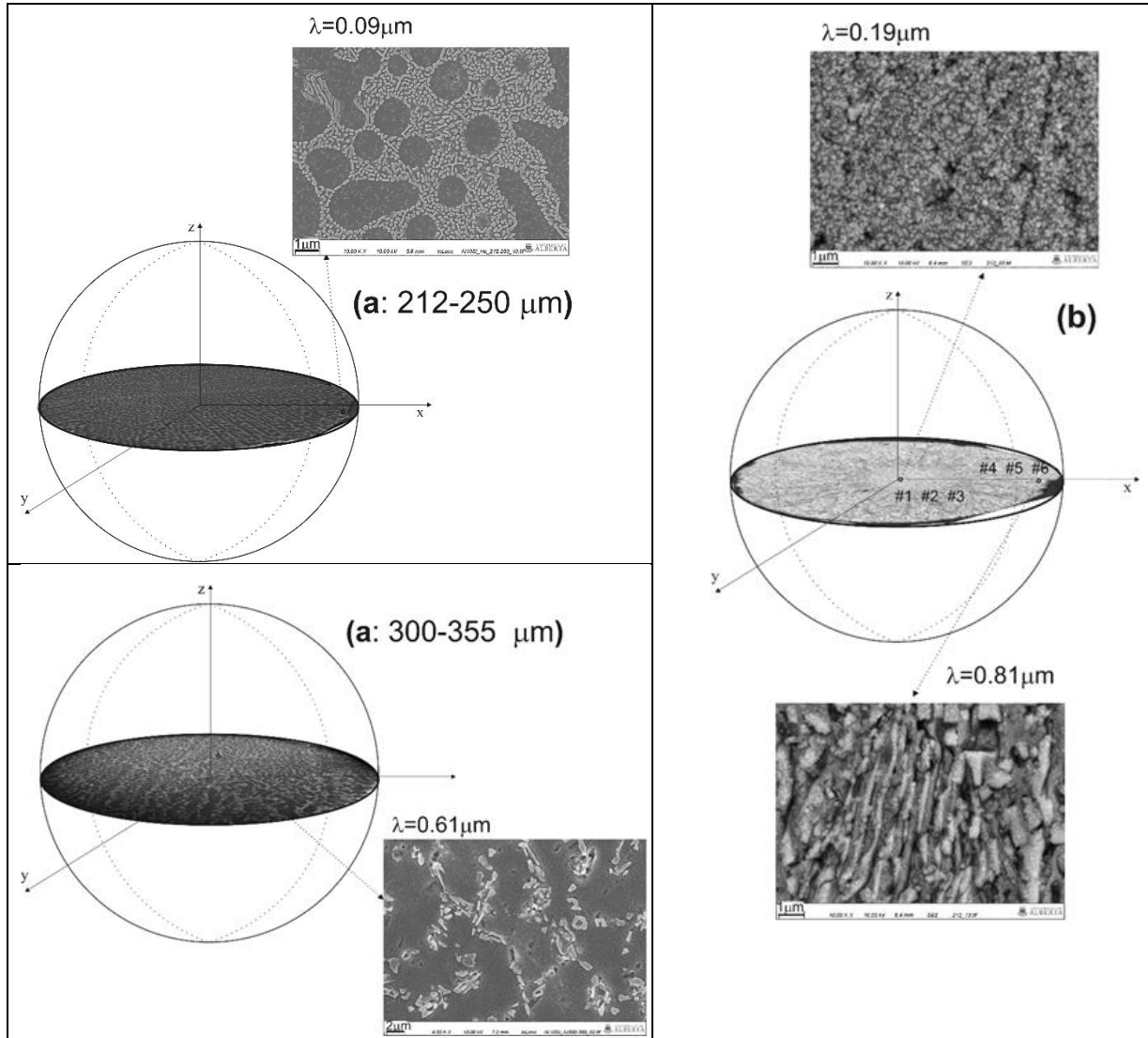


Fig. 6: Typical optical micrographs of cross sections of both Al-10wt.%Si and Al-18wt.%Si powders generated by IA. The variations of the Si morphology and size are shown through SEM images considering (a) two powder sizes (212-250 μm and 300-355 μm) for the Al-10wt.%Si alloy produced in helium and argon atmospheres respectively; and (b) zones A and B of the microstructure associated with the Al-18wt.%Si alloy (212-250 μm in size). λ is the interparticle spacing.

Finally, Fig.7a and Fig.7b show G_E - V_E maps describing the variation of the eutectic Si morphology with cooling rate for both the hypo and hypereutectic Al-Si alloys. It can be seen that high CR and V (low G_E^{-1}) induce globular Si formation. As V decreases the morphology of Si becomes less refined, transitioning from globular to fibrous to flaky. For both compositions there was a region where a mixture of globules and fibers is observed. This seems to be a result of the coalescence of globules while the coalescence of fibers gives rise to flakes, which explains

a region of mixed fibers and flakes. The critical cooling rates for the formation of globular Si are found to be around 800 K/s for Al-10wt% Si and 55 K/s for Al-18wt% Si. This difference could be due to the fact that, for a given powder size, a hyper-eutectic Al-Si alloys yields a higher Si density than as compared to a hypo-eutectic composition, so that the Si growth is restricted in such a way that a cooling rate as low as 55K/s is enough to obtain globular morphologies.

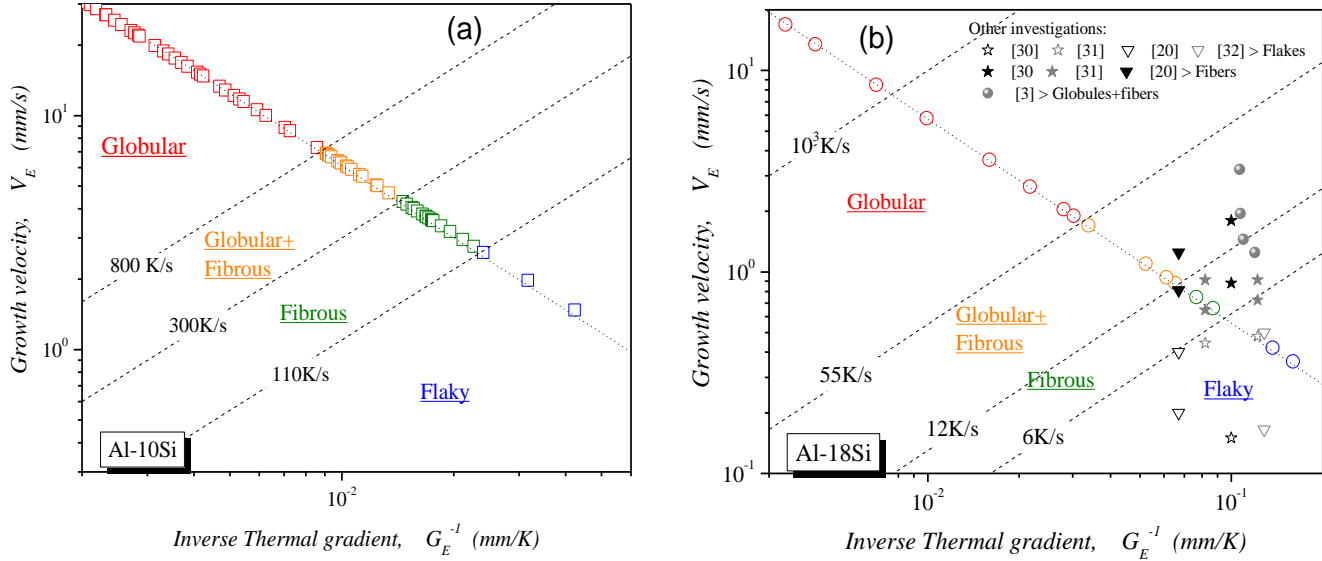


Fig. 7: Diagrams showing maps in G_E - V_E space with the eutectic Si morphology and cooling rate based on IA results for (a) the Al-10wt.%Si and (b) the Al-18wt.%Si alloys, as well as investigations found in the literature [3,20,30,31,32].

4. Conclusions

Rapid solidification of hypo and hypereutectic Al-Si powders generated by Impulse Atomization in argon and in helium atmospheres were investigated. Microstructures development (i.e. scale and morphology) during rapid solidification of the powders was analyzed as a function of estimated eutectic cooling rate and growth rate.

The solidification paths and the resulting eutectic Si morphology in both hypo and hypereutectic Al-Si alloys have been mapped out. Si morphology is found to vary from elongated/fibrous to round/globular as the cooling rate increases.

In the hypo-eutectic composition, the critical cooling rate for the formation of globular Si is found to be 800K/s while in the hyper-eutectic composition, only 55K/s is required to obtain globular eutectic Si. This difference is thought to be due to the fact that, for a given powder size, as compared to a hypoeutectic composition, a hypereutectic Al-Si alloys yields a higher Si density so that the Si growth is restricted in such a way that a cooling rate as low as 55K/s is enough to obtain globular morphologies.

This study suggests that, by making appropriate choices of the solidification parameters, microstructures of Al-Si alloys can be controlled so that the desired globular Si morphology is obtained.

Acknowledgements

The authors are grateful to FAPESP (São Paulo Research Foundation, Brazil: grants 2015/11863-5 and 2016/10596-6) and the Natural Sciences and Engineering Research Council of Canada (NSERC) for their financial support.

References

- [1] Bray, JW (1976) ASM Metals Handbook. Vol.. 2. 10th ed.. ASM Intl..
- [2] Zolotarevsky, VS, Belov, NA, Glazoff, MV (2007) Casting aluminum alloys. Elsevier.
- [3] Reyes, RV, Bello, TS, Kakitani, R, Costa, TA, Garcia, A, Cheung, N, Spinelli, JE (2017) Tensile properties and related microstructures aspects of hypereutectic Al-Si alloys directionally solidified under different melt superheats and transient heat flow conditions. *Mater. Sci. Eng. A.* 685: 235-243.
- [4] Birol, Y. (1966) Microstructural characterization of a rapidly-solidified Al-12wt% Si alloy. *J. Mater. Sci.* 31: 2139-2143.
- [5] Dinda, GP, Dasgupta, AK, Mazumder, J. (2012) Evolution of microstructure in laser deposited Al-11.28% Si alloy. *Surf. Coat. Technol.* 206: 2152-2160.
- [6] Hegde, S, Prabhu, KN. (2008) Modification of eutectic silicon in Al-Si alloys. *J. Mater. Sci.* 43 : 3009-3027.
- [7] Kang, N, Coddet, P, Liao, H, Baur, T, Coddet, C. (2016) Wear behavior and microstructure of hypereutectic Al-Si alloys prepared by selective laser melting. *Appl. Surf. Sci.* 378 : 142-149.
- [8] Shankar, S, Riddle, Y, Makhlof, M. (2004) Nucleation mechanism of the eutectic phases in aluminum–silicon hypoeutectic alloys. *Acta Mater.* 52: 4447-4460
- [9] Kalay, YE, Chumbley, LS, Anderson, IE, Napolitano, RE. (2007) Characterization of Hypereutectic Al-Si Powders Solidified under Far-From Equilibrium Conditions. *Metall Mater Trans A.* 38: 1452-1457.
- [10] Trivedi, R, Jin, F, Anderson, IE. (2003) Dynamical evolution of microstructure in finely atomized droplets of Al-Si alloys. *Acta Mater.* 51: 289-300.
- [11] Pierantoni, M, Gremaud, M, Magnin, P, Stoll, D, Kurz, W. (1992) The coupled zone of rapidly solidified Al-Si alloys in laser treatment. *Acta Metall. Mater.* 40: 1637-1644.
- [12] Nikanorov, SP, Volkov, MP, Gurin, VN, Burenkov, YA, Derkachenko, LI, Kardashev, BK, Regel, LL, Wilcox, WR. (2005) Structural and mechanical properties of Al–Si alloys obtained by fast cooling of a levitated melt. *Mater. Sci. Eng. A* 390: 63-69.
- [13] Olakanmi, EO. (2013) Selective laser sintering/melting (SLS/SLM) of pure Al, Al–Mg, and Al–Si powders: Effect of processing conditions and powder properties. *J. Mater. Process. Tech.* 213: 1387-1405.
- [14] Kang, N, Coddet, P, Liao, H, Coddet, C. (2016) Macrosegregation mechanism of primary silicon phase in selective laser melting hypereutectic Al e High Si alloy. *J. Alloy Compd.* 662: 259-262.
- [15] Magnin, P, Mason, JT, Trivedi, R. (1991) Growth of irregular eutectics and the Al-Si system . *Acta Metall. Mater.* 39: 469-480.
- [16] Wolczynski, W., Billa, B, Rabczak, K. (1996) Interlamellar Spacing in Al-Si Eutectic Growth Controlled by Temperature Gradient. *Mater Sci. Forum* 215–216 (1996) 323.
- [17] Grugel, R, Kurz, W. (1987) Growth of Interdendritic Eutectic in Directionally Solidified Al-Si Alloys. *Metall Trans A.* 18: 1137-1142.
- [18] Jackson, KA, Hunt, JD (1966) Lamellar and rod eutectic growth, *T Metall Soc AIME.* 236: 1129-1142.
- [19] Gunduz, M., Çadirli, E. (2002) Directional solidification of aluminium-copper alloys. *Mater Sci Eng A* 327: 167-185.

- [20] Toloui, B., Hellawell, A. (1976) Phase separation and undercooling in Al- Si eutectic alloy- the influence of freezing rate and temperature gradient. *Acta Metall.* 24: 565-573.
- [21] Wiskel, JB, Henein, H, Maire, E. (2002) Solidification Study of Aluminum Alloys using Impulse Atomization: Part I: Heat Transfer Analysis of an Atomized Droplet. *Can. Metall. Quart.* 41: 97-110.
- [22] Gunduz, M., Çadirli, E. (2002) Directional solidification of aluminium-copper alloys. *Mater Sci Eng A* 327: 167-185.
- [23] Martin, JW, Doherty, RD, Cantor, B. (1997) *Stability of microstructure in metallic systems* Cambridge University Press.
- [24] Angadi, BM, Hiremath, R, Chennakesava, A, Last, R, Kori, SA. (2014) Studies on the Thermal Properties of Hypereutectic Al-Si Alloys by Using Transient Method. *J Mec. Eng. Res Technol.* 2: 536-544.
- [25] Zhang, Z., Bian, X., Wang, Y. Liu, X. (2001) Refinement and thermal analysis of hypereutectic Al-25%Si alloy. *T Nonferr Metal Soc.* 11: 374-377.
- [26] Gündüz, M., Kaya, H., Çadirli, E., Özmen, A. (2004) Interflake spacings and undercoolings in Al-Si irregular eutectic alloy. *Mater Sci Eng A.* 369: 215-229.
- [27] Magnusson, T., Arnberg, L. (2001) Density and Solidification Shrinkage of Hypoeutectic Aluminum-Silicon Alloys. *Metall. Mater. Trans. A.* 32: 2605-2613.
- [28] Brandt, R., Neuer, G. (2007) Electrical resistivity and thermal conductivity of pure aluminum and aluminum alloys up to and above the melting temperature. *Int. J. Thermophys.* 28: 1429-1446.
- [29] Garcia, A, Clyne, TW, Prates, M. (1979) Mathematical model for the unidirectional solidification of metals: 2. Massive molds. *Metall. Trans. B.* 10: 85-92.
- [30] Hosch, T, England, LG, Napolitano, RE. (2009) Analysis of the high growth-rate transition in Al-Si eutectic Solidification. *J Mater Sci.* 44: 4892-4899.
- [31] Khan, S., Ourdjini, A. Hamed, QS, Najafabadi, MA, Elliott, R. (1993) Hardness and mechanical property relationships in directionally solidified aluminium-silicon eutectic alloys with different silicon morphologies. *J. Mater. Sci.* 28: 5957-5962.
- [32] Kaya, H, Çadirli, E, Gündüz, M, Ulgen, A. (2003) Effect of the Temperature Gradient, Growth Rate, and the Interflake Spacing on the Microhardness in the Directionally Solidified Al-Si Eutectic Alloy. *J. Mater. Eng. Perform.* 12: 544-551.